

# Air Effects on Large Droplet Impact

Frank T Smith<sup>1</sup> and Richard Purvis<sup>2</sup>  
*UCL, London WC1E 6BT, UK*

**A study is presented of the interaction(s) between air and water in determining the motion of a large droplet of water, including impacts with a solid surface or with a layer of water. The investigations are partly numerical and partly analytical. They address three main aspects: direct computations for various conditions; analysis of the particular effects of obliqueness at impact; and an approach to capturing the distortion and possible disintegration of a water droplet subjected to significant surrounding air motion.**

## I. Nomenclature

$A$	= magnitude of shear flow in the air
$c$	= ratio $U\delta/V$
$D$	= representative diameter of droplet
$F$	= scaled shape of air-water interface
$F_{st}$	= source term in momentum balance, $\kappa n \delta s / We$
$f$	= interface shape
$f_2$	= perturbation to the interface shape
$\Phi$	= fraction of a cell containing water
$G(T)$	= function of integration
$H$	= water layer depth
$n$	= integer equal to 1 in water, 2 in air
$\underline{n}$	= vector normal to interface
$P$	= scaled pressure variation
$p$	= pressure variation
$q$	= slip velocity at leading order
$Re, Re_1, Re_2$	= Reynolds numbers (globally, in the water and in the air respectively)
$T$	= scaled non-dimensional time
$t$	= non-dimensionalised time
$U$	= (constant) horizontal velocity component of the incoming droplet
$V$	= (constant) vertically downward velocity component of the incoming droplet
$u, v$	= velocity components in $x, y$ directions respectively
$u_1, v_1, p_1$	= scaled contributions to $u, v, p$ in the water
$u_2, v_2, p_2$	= scaled contributions to $u, v, p$ in the air
$u_\infty$	= far-field velocity component in air flow
$\underline{u}$	= velocity vector
$We$	= Weber number
$X, Y, y_2$	= scaled horizontal or vertical Cartesian coordinates
$x, y$	= horizontal and vertical Cartesian coordinates, non-dimensionalised

<sup>1</sup> Goldsmid Chair, Mathematics Department, UCL, Gower Street, London, WC1E 6BT, UK.

<sup>2</sup> New position: Lecturer, School of Mathematics, UEA, Norwich, NR4 7TJ, UK.

$\delta$	=	aspect ratio of the air layer
$\delta x$	=	spatial grid step
$\delta_s$	=	delta function concentrated on interface
$\kappa$	=	mean curvature
$\mu_1, \mu_2$	=	viscosity in water and air, respectively
$\nu_1, \nu_2$	=	kinematic viscosity in water and air, respectively
$\rho_1, \rho_2$	=	density in water and air, respectively
$\tau$	=	scaled interfacial shear stress

## II. Introduction

THE first aim, in this continuing work on air effects during large droplet impact, is to enhance the understanding of the influence of splashing on the formation of ice on a wing, in particular for super-cooled large droplets where splash appears to have a significant effect along with the influence of surrounding air motion. To date, there has been relatively little direct theoretical input and suitable physical modelling on droplet impact, in particular concerning air-water interaction, not to mention mass and heat transfer and the relationship between input and rebound droplets. The impact of a single droplet onto an otherwise undisturbed layer of water, with air effects present, is examined here. Analytical and computational approaches are used as in Refs. 1-6.

The flow for small times after impact can be determined analytically, for direct and oblique impact and for a deep or a shallow layer. The impact can also be examined numerically using the VOF (volume of fluid) method, initially treating the fluid as inviscid and incompressible; at small times there are promising comparisons with the analytical solution and with some experimental work capturing the ejector sheet <sup>2,5</sup>.

The numerical method and some accompanying analysis may likewise be used to consider cases corresponding to varying the layer depth to droplet diameter ratio, the influence of surface tension and oblique impact, focussing on what effect they have on the form of splash produced, the geometry of the crown formed and the make-up of the ejected droplets. In particular the amount of rebounded fluid is examined. Although thermal effects are not included in the current work emphasis is also placed upon the exchange of fluid, tracking the pre-existing (warmer) layer fluid and the (colder) incoming droplet fluid and considering the proportions of each in the splash. This exchange can have a great influence on the overall temperature of the water layer. The influence of an ice shape beneath the water layer can be modelled and the effects of its presence on the rebound and the constituents of the ejected fluid are able to be explored. See also Refs. 1-6.

Second, however, a major and complex aspect in all this is the effect of the surrounding air motion. This concerns in particular pre-impact and post-impact air cushioning and pre-existing airflow, and the parts played by the extreme viscosity and density ratios. An approach aimed at dealing with the distortion and possible disintegration of a water droplet surrounded by air flow will be presented.

The paper is arranged as follows. Section II below describes recent computational results using a VOF method to tackle the effects of air flow on a droplet motion, and vice versa, with or without an impact taking place. Section III is concerned with analytical or reduced-equation theory and results on air flow effects associated with impact processes either immediately before or immediately after an impact. The effects of an oblique approach can be significant in industrial terms and so these are incorporated whereas other important effects such as from gravity, surface tension and compressibility are examined in the literature. Section IV moves on to describe air flow effects and their two-way interaction with the water droplet behaviour far from impact, where shape distortion and possible disintegration of the droplet are of prime interest. Section V presents final comments. *The non-dimensionalization* and the Reynolds number  $Re$  are based on the vertical component  $V$  of the droplet approach velocity, on a typical droplet diameter, on the density  $\rho_1$  of the water (or fluid 1), and on the kinematic viscosity  $\nu_1$  in the water, while the pressure is measured relative to the atmospheric value. The coordinates and time are centred near the area and instant of impact. The starting point is the Navier-Stokes equations, which are, with  $\Delta$  denoting the Laplacian,

$$\underline{u}_t + (\underline{u} \cdot \underline{grad}) \underline{u} = - (\rho_1 / \rho_n) \underline{grad} p + (\rho_n / \rho_1) Re^{-1} \Delta \underline{u} \quad (1.1)$$

both in the water, with subscript  $n = 1$ , and in the air (fluid 2) with  $n = 2$  where the air density and kinematic viscosity are  $\rho_2, \nu_2$  in turn. The continuity equation  $\text{div } \underline{u} = 0$  applies in each fluid.

### Numerical results on air-flow effects

In VOF modelling of the effect of airflow on splashing previous studies<sup>1, 2</sup> have considered the impact of a droplet onto a thin liquid film in a vacuum and in air. However, previously the air, if present at all, has been assumed to be still initially. In this section we describe some initial results examining the possibility of inclusion of an air flow in the model. This is a physically important case as understanding where the splashed liquid mass goes after being ejected is important in aircraft icing; it determines whether water re-impinges, changing the ice shape, or escapes, changing the ice mass. Of course, in an actual icing situation the airflow is very dependent on the local geometry. Here we investigate some idealised air flows to try to obtain some tentative understanding as to how a cross-flow influences the splash.

With the numerical method adopted here, a VOF approach, one of the major difficulties with solving the current problem numerically lies in coping with the change in topology as the droplet enters the layer and secondary droplets are subsequently ejected. The VOF method can in principle handle such surface reconnection and breakup without any special treatment or catastrophic break down and so it was thought suitable for our use. The method was first introduced by Refs. 7-9 and has been honed and improved upon since then by several authors, for example Ref. 10, and in particular in Ref. 11 where it has applied to droplet impacts. We shall give a brief overview here.

The main idea behind the VOF method is to track the position of the interface by use of a function  $\Phi$  representing the fraction of a given grid cell that is filled with fluid. In other words we introduce a function  $\Phi$  which takes the

$\Phi = 1$  if cell is full of water

$\Phi = 0$  if cell is full of air

$\Phi =$  fraction of cell containing water (2.1)

values

in each grid cell. As such we have  $0 < \Phi < 1$  in cells containing the free surface. To ensure the free-surface moves

$$\frac{\partial \Phi}{\partial t} + (\underline{u} \cdot \text{grad}) \Phi = 0, \tag{2.2}$$

with the fluid the function  $\Phi$  satisfies the evolution equation

where  $\underline{u}$  is the velocity vector determined from solving the flow in the main body of the fluid.

Introducing  $\Phi$  allows us to keep track of the free surface and follow it in time but in doing so we lose our knowledge of the exact position of the free surface; this needs to be inferred from the volume fractions. The reconstruction of the interface can be performed in a variety of ways, from the straightforward

step-stair or SLIC

methods<sup>8</sup>, which force the free-surface to align with the x and y coordinates in each grid cell, to one of various piecewise linear (PLIC) methods. The latter constructs the interface by estimating the normal vector to the actual free surface in each grid cell and reconstructing the interface as the straight line which, with the same normal, encloses the correct amount of fluid F. The PLIC method gives much better resolution than the simple but relatively crude SLIC methods; it is the PLIC method that we have adopted. See Ref. 10 for further details and comparisons. Equations (1.1) govern the flow in the fluid, subject to carefully applied boundary conditions at the free surface, and the system is solved using the SIMPLE algorithm. Surface tension is included using an approach called the continuous surface force (CSF) method: see Ref. 12 and references therein for details. This models the surface tension by including a source term  $\underline{E}_{st}$  in the right-hand side of the momentum equations. This term is defined by

$$\underline{E}_{st} = \kappa \underline{n} \delta_s / We, \quad (2.3)$$

where  $\kappa$  is the mean curvature,  $\underline{n}$  is the normal and  $\delta_s$  is a delta function concentrated on the interface. It should be noted however that the method becomes unstable for cases with surface tension that use a realistic density ratio between the water and the air. For example Ref. 15 and references therein use dense air (pseudo-air) in order to be able to cope with surface tension. Here we have used an accurate water-air density ratio and excluded surface tension. Some examples were run including surface tension but were found to be unstable.

The grid size is typically taken as  $\delta x = 0.01$  in both the x and y directions. This choice of grid size was checked by using finer grids; the results were found to be indistinguishable from those presented here. The domain size was taken as a compromise between allowing a substantial part of the splash to be seen and having a reasonable run time for the code. The boundary conditions on the side and upper edges of the domain are in effect porous, such that the fluid can pass through them.

Figures 1-3 show three sample cases of droplet impact with pre-existing air flow, the two fluids being taken as inviscid in these calculations. The imposed air flow in each case is a simple shear flow  $u=A(y-H)$ , of varying magnitude A. In each case the air flow is from left to right and the evolution of the splash is shown at four specific

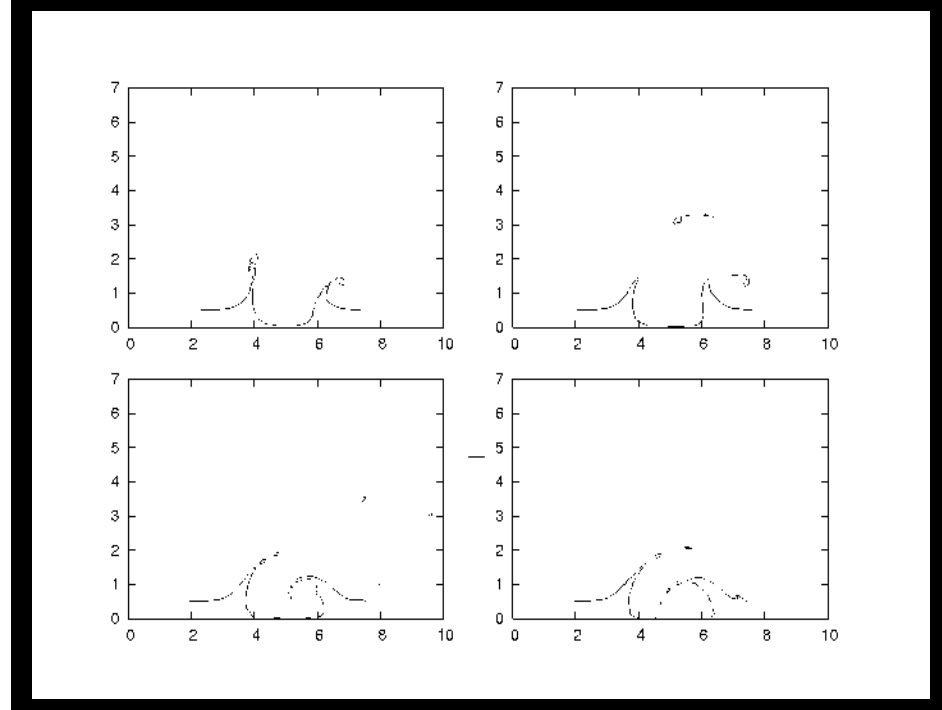
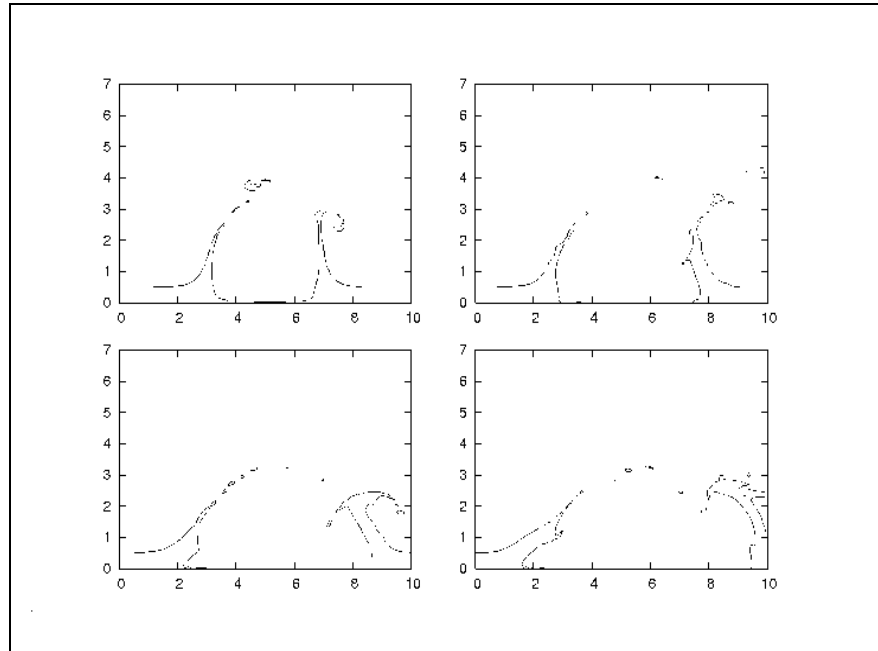


Figure 2. Case D/H = 1, with uniform shear factor A = 0.1 in the air flow.

time steps. The first figure shows a case with  $D/H=4$  (a comparatively large droplet) and a relatively low imposed air velocity, with  $A$  being a tenth of the incoming droplet velocity. At early times there is little asymmetry, although the left-hand part of the corona breaks up into droplets first. Then, as the crown enters the more severe air flow the ejected droplets are swept away. The right-hand part of corona collapses outwards. The second figure is for a medium-sized droplet  $D/H=1$  but with the same air velocity. Here, with a less significant corona



**Figure 3. Case  $D/H = 4$  but with uniform shear factor  $A = 0.5$  in the air flow.**

generated by the medium-sized incident droplet, a few sub-droplets are swept away but almost all of the splash collapses back into the water layer close to the point of impact. Finally in Fig. 3 we again have  $D/H=4$  (comparatively large droplet) but now with  $A$  increased to be equal to half the incoming droplet velocity. Again all the ejected droplets get swept away, but this occurs earlier compared with the previous two configurations due to the increased air velocity here, and the water does not reach as great a height compared with the case with a lower  $A$  value.

It should be noted that many other examples have not yet been amenable to this approach; for some configurations, particularly for larger droplets or stronger cross flow but also for parameters within the range displayed here, the method has so far failed to converge. These difficulties tend to suggest the additional /complementary use of analytical approaches such as those considered in the next sections.

### Analysis on air effects near impact

This section concerns results from analytical methods based on reduced-equation modelling to allow for air flow effects especially at or near the time of a single impact of a droplet onto a water layer or a solid surface. Recent work

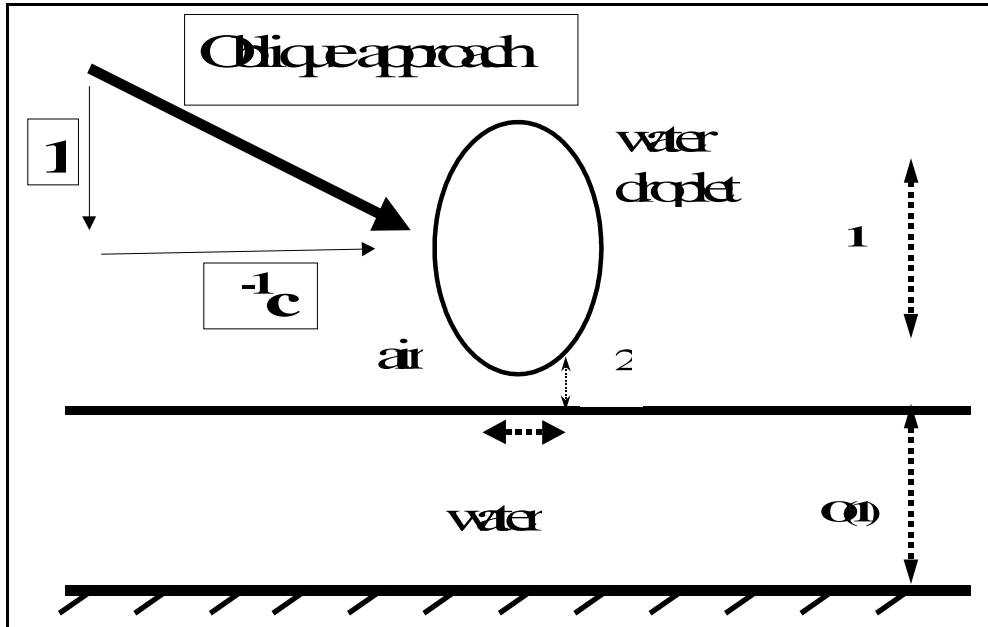


**Figure 4. Diagram of oblique impact involving water droplet, air and water/solid surface. The approach velocity components of the droplet shown in boxes should be 1 and  $\delta^1 c$ . The local length scales induced should read  $\delta$  horizontally and  $\delta^2$  vertically.**

is in Refs. 3,4,6.

Regarding air effects and *obliqueness* effects on impacts, a main issue concerns when and how substantial air-water interaction first occurs near the oblique impact of a water droplet onto a flat horizontal fixed solid surface (wall) or another body of water, with air in-between, as in Fig.4. The impact then has rapid local interaction involving the thin air layer.

The present theory now takes the density and viscosity ratios  $\rho_2 / \rho_1$ ,  $\nu_2 / \nu_1$  of the two fluids 1, 2 to be small: for dry air with pure water these two ratios are near 1/828 and 1/55 in turn, at 20 degrees C and one-atmosphere pressure. We stress that viscous forces are included in the present theory. Near impact, as the aspect ratio of the air layer becomes small, the length scalings of that layer are  $(x, y) = (X, \delta^2 y)$  in view of the droplet's  $O(1)$  curvature, whereas the length scalings in the water are  $(X, Y)$ . An order of magnitude argument therefore suggests

$$(u, v, p) = (\delta^1 c + u_2, v_2, \delta^1 p_1) + \dots \text{ in the water,} \quad (3.1a)$$

$$(u, v, p) = (\delta^1 u_2, v_2, \delta^1 p_2) + \dots \text{ in the air} \quad (3.1b)$$

based on the kinematic and pressure conditions at the unknown interface and on Eq. (1.1) along with continuity, with the typical time scale  $t = \delta^2 T$  being short. The size  $\delta^1 c$  of the relative incident horizontal velocity component  $U/V$  (see also Fig. 4) of the droplet is such as to significantly affect the local interaction. The governing equations in the air are of thin-layer type. In fact the individual contributions in Eq. (1.1) for  $n = 2$  are now of order  $\delta^{-3}$  [from acceleration],  $\delta^{-3}$  [inertia],  $\delta^{-2} (\rho_1 / \rho_2)$  [pressure gradient],  $(\nu_2 / \nu_1) \text{Re}^{-1} \delta^{-5}$  [viscous] in the x direction and all are in balance if  $\text{Re} \sim (\rho_2 / \rho_1) \delta^{-2}$  and  $(\nu_2 / \nu_1) \sim \delta^2 y$  elding

$$\text{Re} \sim (\rho_2 \delta^2) / (\nu_1 \delta^2). \quad (3.2)$$

Hence the air-water interaction is controlled by the coupled system of the unsteady boundary layer equations in the air along with

$$(\partial_T + c \partial_X)^2 F = -1 (P.V.) \int P_s(s, T) (X-s)^{-1} ds \quad (3.3)$$

from the unsteady potential flow in the water, where the principal value integral extends from minus infinity to plus infinity. The unknown pressure P stands for  $p_1$  evaluated at Y zero and is identical to  $p_2$ . The boundary conditions include the kinematic condition on  $v_2$  and a matching constraint  $u_2 = c$  at the unknown scaled interface  $y_2 = F$ , as well as no slip at  $y_2$  zero.

The estimate in Eq. (3.2) acts as a critical Reynolds number and its value is about  $10^7$  for water with air. Because of the industrial setting<sup>1-6, 13</sup> where typical Re values of  $10^4$  to  $10^5$  are encountered there is much interest in the subcritical range. There the air equations and the appropriate boundary conditions reduce to the Reynolds

$$(F^3 P_X)_X = 12 (F_T + c F_X/2) \quad (3.4)$$

lubrication equation

in normalised form. So far the working is for oblique droplet impact onto a fixed solid but essentially the same system of Eqs. (3.4), (3.5) applies for impact onto water<sup>3, 4, 6</sup>. Also, equivalent equations hold in a frame moving with the horizontal velocity U of the droplet where the wall appears as an upstream-moving wall<sup>3, 6</sup>.

Computational solutions of Eqs. (3.3), (3.4) were obtained by adapting a numerical method from previous papers<sup>3, 4, 6</sup>, which address the case of zero  $c$  (normal impact). Grids and time steps similar to those used in these papers were applied here as well and tested satisfactorily for accuracy. The initial conditions and the far-field boundary conditions are those of an approaching parabola shape  $(X-cT)^2 - T$  for  $F$ , corresponding to the lower

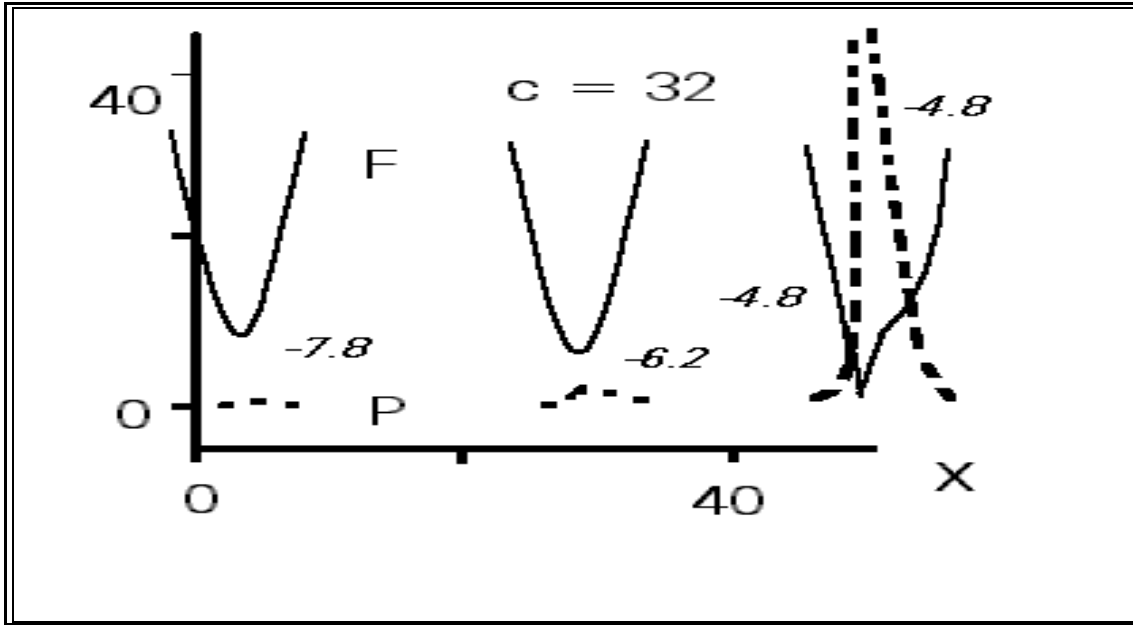


**Figure 5. Droplet interface shapes  $F$  (solid) and pressures  $P$  (dashed) plotted against  $X$ , near impact for an angle of obliqueness corresponding to  $c = 32$ , at the scaled times marked.**

reaches of the smooth total incoming droplet, and of negligible induced pressure ( $P$  tending to zero) which is associated with the atmospheric pressure holding outside the interaction region. The results for two different positive values of  $c$  are shown in Ref. 6 and one (for  $c = 32$ ) in Fig. 5 and they indicate effects not dissimilar to those of inclined gravity<sup>3, 6</sup>. A skewed touchdown ( $F$  tending to zero) is indicated generally at negative  $T$ ; thus the presence of air hastens touchdown. This is in the fixed frame, note, with a relatively high incident horizontal velocity component, and the angle of approach measured from the horizontal is  $V/U$ , i.e.  $\delta / c$ . In the extreme of large  $c$  the majority of the solution has  $T \propto c$  and enlarged lengths  $X-cT \propto c^{1/2}$ , so that in a moving frame the right side of Eq. (3.4) approaches  $-6c F_x$ ; Eq. (3.4) now integrates to give  $F^3 P_x$  as  $-6c F + G(T)$ . Here  $G$  must be nonzero to give zero farfield  $P$ . Substitution into Eq. (3.3) to yield an  $F$  equation then suggests that the  $G$  term drives the touchdown process, in which the minimum  $F$  tends to zero in a square-root manner in scaled time.

More widely, the results also prompt thoughts on pre-existing air flow effects since we would expect such air flow also to provoke skewing, for example by means of an extra streamwise mass flux. Analysis for large negative  $T$  however suggests that, at least for zero  $c$ , skewing is present only if the incident shape is already skewed. This is because the farfield  $P$  must be zero. Solutions with such incident skewing are included in Ref. 3. With nonzero  $c$  an extra mass flux is induced but it is a definite amount rather than arbitrary. In fact, skewing of the incident shape may well be how pre-existing air flow influences the impact process in practice, by altering the droplet shape considerably before the local interaction comes into play. This brings us to the next section.

The work above and in Refs. 3, 4, 6 has mostly been on pre-impact interactions involving air effects. Post-impact behaviour is also discussed in Ref. 4. In particular it is found that sufficiently strong air flow can disrupt the structure of the rapidly spreading droplet motion on the solid surface or water layer after impact, as well as producing a significant decrease of the droplet spreading rate. The disruption can be so severe that complete restructuring occurs locally.



#### IV. Droplet distortion by airflow: small-density-ratio small-viscosity-ratio theory

Distortion and even subsequent disintegration of sufficiently large droplets are of much concern prior to impact because they affect the nature and number of splashes produced by impacts<sup>14, 15</sup>. They are also of interest after impact. Distortions and disintegrations pose difficult tasks computationally however due to the need to cope with the small ratios of density and viscosity for air and water as well as strong or severe distortions of shape; see also Section II. That very smallness of the ratios raises the possibility of analytical progress, as a complementary approach, based on those ratios being major parameters in a fashion similar to that explained in the previous section. Successful use of such an approach has been seen in the work of Refs. 3, 4, 6 described earlier on for other droplet situations, while one-sided approximations adopted in other fields, e.g. Ref. 16, including even the classical free-surface approach in a sense, represent yet other uses. Here we describe the beginnings of a small-ratio approach applied to droplet distortion first of all far from impact.

The planar distortion theory proceeds as follows, from the governing equations (1.1), with  $\rho_2/\rho_1$  again assumed to be  $O(1)$  typically and with  $Re$  also regarded as  $O(1)$  for now. Thus again viscous forces are incorporated. Both  $\rho_2/\rho_1$  and the viscosity ratio  $\mu_2/\mu_1$  are now  $O(\epsilon)$  say, where  $\epsilon$  is small. See Fig. 6, where  $u_\infty$  represents the imposed air velocity of  $O(1)$  in the far-field. Suppose that the representative velocities  $|\underline{u}|$  in both the water droplet and the surrounding air are of  $O(1)$ . Thus the flow solution expands in the form

$$(\underline{u}, p) = (\underline{u}^{(a)}, \epsilon p^{(a)}) + \epsilon (\underline{u}^{(b)}, \epsilon p^{(b)}) + \dots \text{ in the air, and } (\underline{u}, p) = (\underline{u}^{(b)}, p^{(b)}) + \dots \text{ in the water.} \quad (4.1)$$

Then assuming appropriate initial conditions the solution procedure is: (i) solve Eq. (1.1) in the water subject to zero normal stress (or approximately pressure  $p$ ), zero tangential stress ( $\tau$ ) and the kinematic condition on the interface  $y = f(x, t)$ , in order to determine  $f$  (or rather  $f^{(a)}$ ) and the slip velocity  $q(x, t)$  on it; (ii) solve Eq. (1.1) in the air with  $f, q$  as given, the normal velocity being given by the kinematic condition, in order to determine  $p$  and  $\tau$ , both of these quantities being of order  $\epsilon$  from Eq. (1.1); (iii) feed the  $O(\epsilon)$  corrections for  $p, \tau$  into the calculation in (i), to produce a correction  $f^{(b)}$  to  $f$ , and continue.

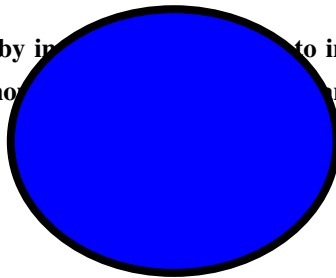
Suppose instead however that  $|\underline{u}|$  is small in the water droplet, at least initially, whereas in the surrounding air  $|\underline{u}|$  is of  $O(1)$ . This seems at first merely a special case of that above but it throws up interesting physics and

$$(\underline{u}, p) = (\underline{u}^{(a)}, \epsilon p^{(a)}) + \dots \text{ in the air, but } (\underline{u}, p) = \epsilon (\underline{u}^{(b)}, p^{(b)}) + \dots \text{ in the water.} \quad (4.2)$$

appears to represent well the typical droplet scenario. Here the flow expansion is

Then part (i) above has  $\underline{u}, p$  identically zero and say a steady circular shape for  $f$  as a start, although other fixed shapes are possible. Part (ii) now becomes the classical problem of determining the evolution of motion past a fixed circular cylinder subject to no slip at the surface, for finite  $Re = Re_2$ , producing  $p, \tau$ . Part (iii) becomes the task of

**Figure 6. On droplet distortion by incident air stream in the x direction. The density and viscosity of the air show  $\rho_1, \mu_1$  and for water  $\rho_2, \mu_2$ .**



determining the linearized flow inside the cylinder with given  $p, \tau$  at the known surface; the kinematic condition acts to yield the  $O(\epsilon)$  correction  $\epsilon f^{(b)}$  to  $f$  almost as an afterthought. The linearized version of Eq. (1.1) implied in part (iii) should enable the evolution to be much more tractable. The classical form of part (ii) potentially has a similar advantage.

Continuation of the theory is likely to involve the following points.

A) The influence of surface tension effects can be built into the model by means of the non-dimensional pressure jump at the unknown interface where

$$p_1 - p_2 = \kappa / We \tag{4.3}$$

in normalised form. The interfacial curvature  $\kappa$  is expected to be  $O(1)$  in general, initially at least, whereas  $We$  can be anything from  $O(1)$  to large of the order  $10^4$  to  $10^5$  in practice, depending on the precise setting. Thus  $1 / We$  can reasonably be taken to be  $O(1)$ , or to be comparable with the typical density ratio  $\epsilon$ , in which case the surface tension effects might, but usually do not, matter in the dynamics above, or can be deemed significantly smaller than

$\epsilon$ , in which case the surface tension for certain does not matter substantially. Moreover a starting state in which the pressure  $p_1$  say is constant would be consistent with the starting shape of the droplet being circular, in view of the curvature term in Eq. (4.3), for any size of  $1/We$ .

B) Likewise the relative effect of gravity is of the order of the inverse Froude number, that is about  $10^{-7}$  in reality here. This may be either assumed as being comparable with the density ratio  $\epsilon$  or taken as relatively small.

C) The influence of a wall (for example a wing surface) approaching the droplet can be accommodated, in essence as a prescribed far-field velocity for the air motion but accompanied by the presence of a moving wall, in the coordinate frame of the droplet. A sample first approximation to such a far-field velocity is one directed in the negative  $x$  direction such that

$$u_{\infty} = - \exp(x + t - c) \text{ in the air region, where } x < c - t. \quad (4.4)$$

Here the leading edge surface of the wing (as if incoming from the right in Fig. 6) is positioned at  $x = c - t$ , for times such that  $t < c$ , while the droplet is virtually still at  $x = 0$  for some time range at least. The incoming solid surface, on which  $u$  must be equal to  $-1$  in this case, is supposed as flat here for convenience.

D) Solution properties for the scenario of Eq. (4.2) would be of interest at small  $t$ , at  $Re$  values of order unity or at extreme  $Re$ , especially as the induced surface shears increase in magnitude, at large  $t$ , and so on.

E) At large  $t$  interfacial instabilities such as the Rayleigh-Taylor and other ones may emerge, but there is the intriguing possibility that  $f_2$  simply increases in proportion to  $t$ , in order to keep the kinematic condition satisfied within the water droplet during the dynamics of part (c) above. If so, then a new time scale comes into operation, when  $t$  is considerably larger, of the order  $1/\epsilon$ . At that stage the air-water behaviour is quasi-steady but fully nonlinear as the interface then becomes severely distorted.

F) The same ideas apply for the modelling of three-dimensional distortions.

## V. Further comments

A study has been presented concerning the interactions between air and water in determining the motion of a large droplet of water, including impacts with a solid surface or with a layer of water. The investigations involved in the study have been partly numerical and partly analytical. They have addressed three main aspects. These are, first, direct computations for various conditions as described in Section II; then an analysis in Section III on the particular effects of obliqueness at impact; and third a theoretical approach to capturing the distortion and possible disintegration of a water droplet subjected to significant surrounding air motion, as presented in Section IV. Given the complexity of the dynamics in air-water interplay, the numerical and analytical contributions here are intended to be complementary. The extension to three-dimensional interactions would be potentially very interesting as well as useful.

## Acknowledgements

We thank EPSRC and QinetiQ for support through the Faraday Partnership for Industrial Mathematics, managed by the Smith Institute, and also David Allwright, Roger Gent, Geoffrey Luxford, David Hammond, Richard Moser, Manolo Quero and Paul Spooner for their interest and helpful discussions.

## References

- <sup>1</sup>Purvis, R, and Smith, F. T., "Large droplet impact on water layers," *AIAA paper 2004-0414*, 2004, presented at 42<sup>nd</sup> Aerospace Sci Conf & Exhib, Reno NA, January 5-8, 2004.
- <sup>2</sup>Purvis, R, and Smith, F. T., "Droplet impact on water layers: post-impact analysis and computations," *Phil Trans Roy Soc A*, 2006, in press.
- <sup>3</sup>Smith, F. T., Li, L. and Wu, G.-X., "Air cushioning with a lubrication /inviscid balance," *J Fluid Mech*, vol. 482, 2003, pp. 291-318 .
- <sup>4</sup>Smith, F. T. and Purvis, R., "Air-water interactions near droplet impact," *Europ J Applied Math*, vol. 15, 2005, pp. 1-19.

- <sup>5</sup>Howison, S. D., Ockendon, J. R., Oliver, J. M., Purvis, R. and Smith, F. T., “Droplet impact on a thin fluid layer,” *J Fluid Mech*, 2006, submitted
- <sup>6</sup>Smith, F. T., Ovenden, N. C. and Purvis, R., “Industrial and biomedical applications,” in *One Hundred Years of Boundary Layer Theory*, 2006, eds. G. E. Meier & K. R. Sreenivasan, Kluwer Academic Publications, in press.
- <sup>7</sup>DeBar, R., “Fundamentals of the Kraken code,” *Technical Report*, UCIR-760, LLNL, 1974.
- <sup>8</sup>Hirt, C. W. and Nichols, B. D., “Volume of fluid (VOF) method for the dynamics of free boundaries,” *J Comp Phys*, vol. 39, 1981, pp. 201.
- <sup>9</sup>Noh, W. F. and Woodward, P. R., “SLIC (simple line interface method),” in *Lecture Notes in Physics*, vol. 59, 1976, pp. 330.
- <sup>10</sup>Rider, W. J. and Kothe, D. B., “Reconstructing volume tracking,” *J Comp Phys*, vol. 141, 1998, pp. 112-152.
- <sup>11</sup>Gueyffier, D., Li, J., Nadim, A., Scardovelli, R. and Zaleski, S., “Volume-of-fluid interface tracking with smoother surface stress methods for three-dimensional flows,” *J Comp Phys*, vol. 152, 1999, pp. 423-456.
- <sup>12</sup>Scardovelli, R. and Zaleski, S., “Direct numerical simulation of free-surface and interfacial flow,” *Ann Rev Fluid Mech*, vol. 31, 1999, pp. 567-603.
- <sup>13</sup>Gent, R. W., Dart, N. P. and Cansdale, J. T., “Aircraft icing,” *Phil Trans Roy Soc A*, vol. 358, 2000, pp. 2873-2911.
- <sup>14</sup>Luxford, G., Hammond, D. W. and Ivey, P., “Modelling, imaging and break-up of distortion, drag and break-up of aircraft-icing droplets,” *AIAA paper 2005-0071*, 2005, presented at 43<sup>rd</sup> Aerospace Sci Conf & Exhib, Reno NA, January 10-13 2005.
- <sup>15</sup>Josserand, C. and Zaleski, S., “Droplet splashing on a thin liquid film,” *Physics of Fluids*, vol. 15, 2006, pp. 1650-1657.
- <sup>16</sup>Davis, S. H., “Interfacial fluid dynamics,” in *Perspectives in Fluid Dynamics*, ch. 1, 2000, pp. 1-51, Cambridge University Press.